



9th Euroconference on Rock Physics and Geomechanics

Trondheim Norway 17-21 October 2011

Experimental investigation of the delayed behaviour of the unsaturated argillaceous rocks by means of Digital Image Correlation techniques

D.S. Yang, M.Bornert, S. Chanchole,
L.L. Wang, and P. Valli

Laboratoire de Mécanique des Solides
Laboratoire Navier

I. Introduction

- Argillaceous rocks of Meuse/Haute Marne
- Hydromechanical behavior of argillaceous rocks at various scales
- Object

II. Multiscale full-field strain measurements

- Experimental setup
- Digital image correlation (DIC) and systematic errors
- Strain measurement accuracy

III. Hydromechanical behavior of argillaceous rocks

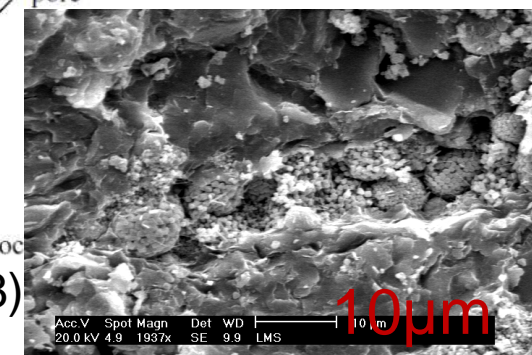
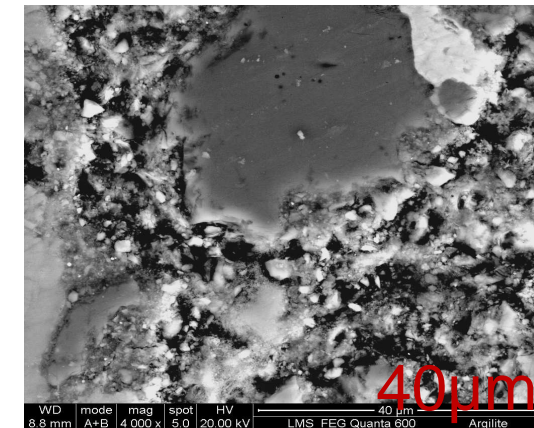
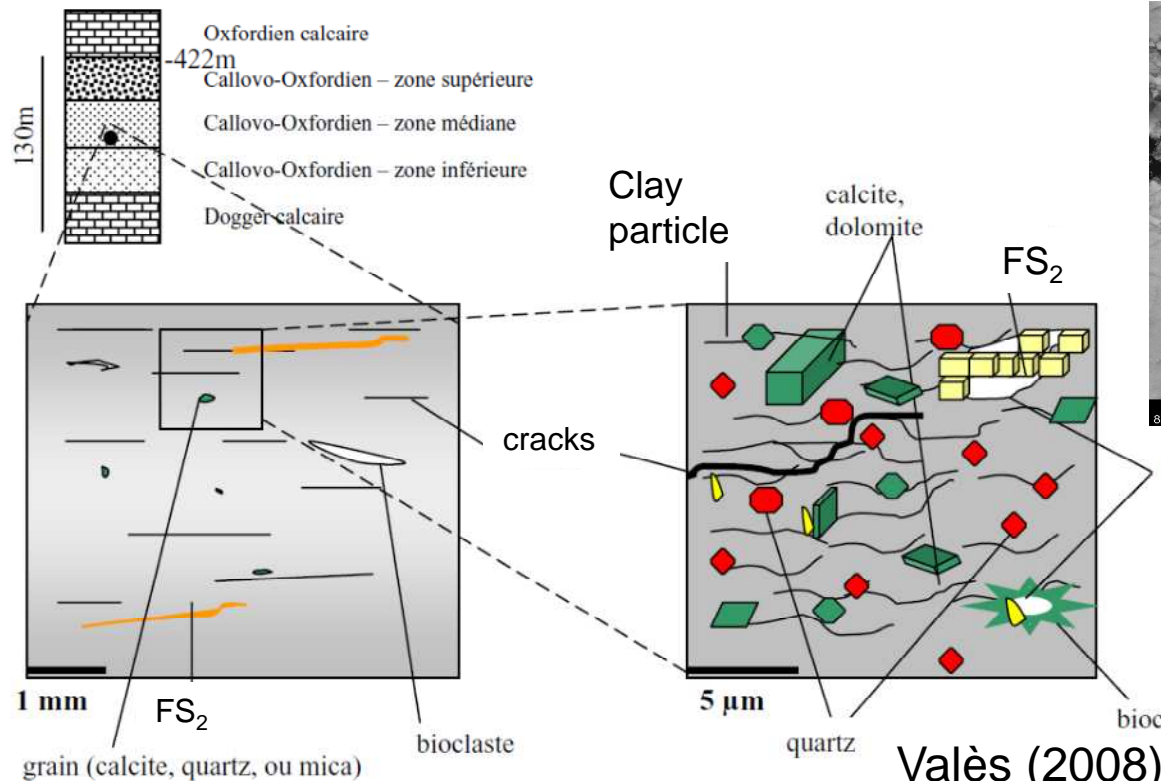
- Hydration and dehydration under uniaxial loading
- Creep behavior under controlled HM

IV. Conclusions

Argillaceous rocks of Meuse/Haute Marne

Depth: -420 et -550 m (130 m thick)

Mineralogy: clay minerals (~45%); carbonates (~20%); quartz (~30%)



Valès (2008)

Total porosity :

15%

Permeability :

$<10^{-20} \text{ m}^2$

Hydromechanical behavior of argillaceous rocks

Shrinking and Swelling: strain related to RH

E and Rc ↘, when RH ↗

Creep : more significant, when RH ↗

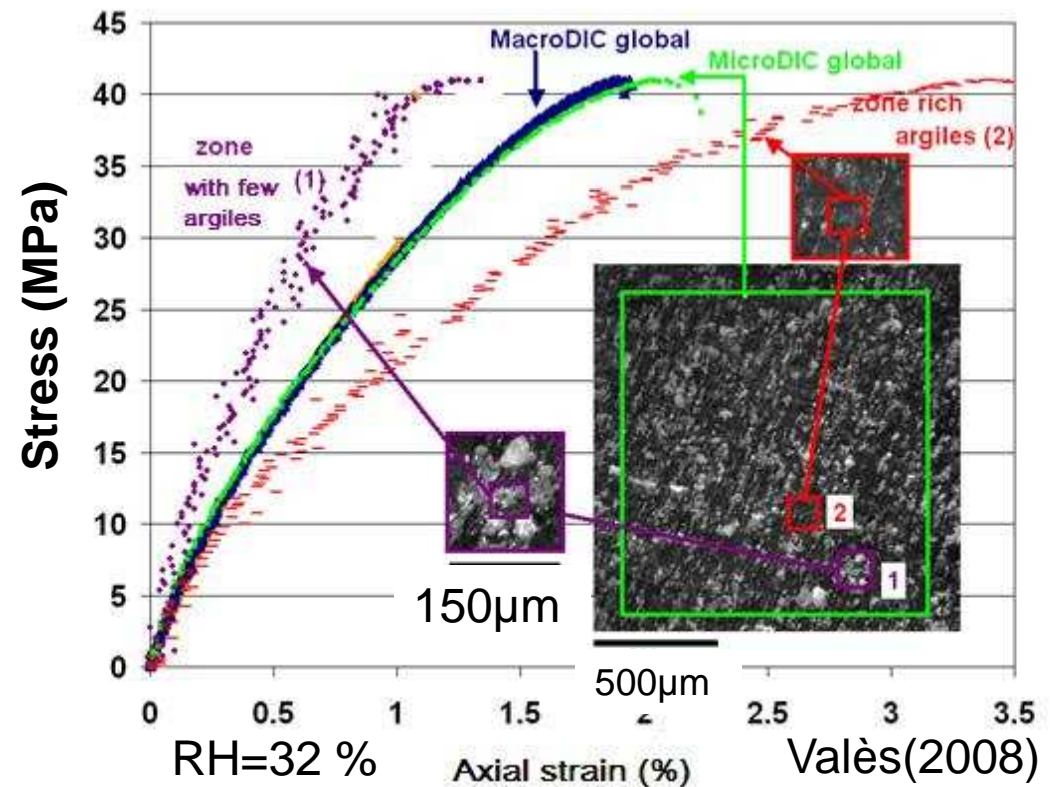
10^{-4} / ° RH

10^{-2} $\epsilon_{rupture}$

10^{-4} / week

Microstructure induces heterogeneous mechanical response at various scales

Reversible, irreversible,
elastic, plastic, creep,
hydration ... :
at which scale? RVE?



Object

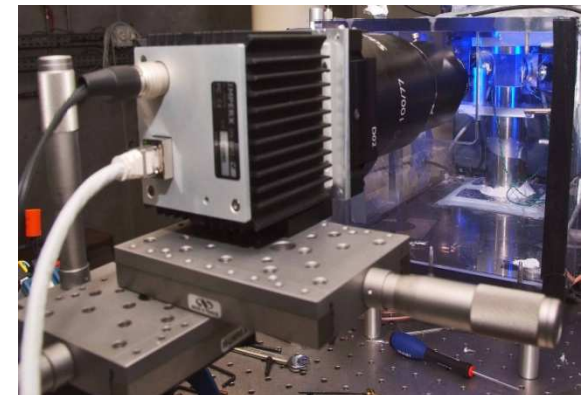
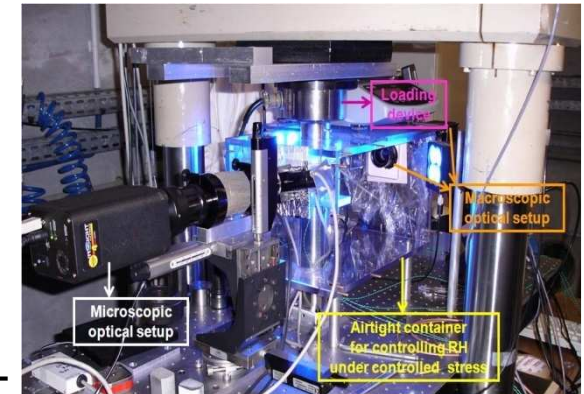
**Study of the mechanisms of delayed behavior
of the argillaceous rocks
under coupled HM conditions**

By means of DIC technique

Experimental setup

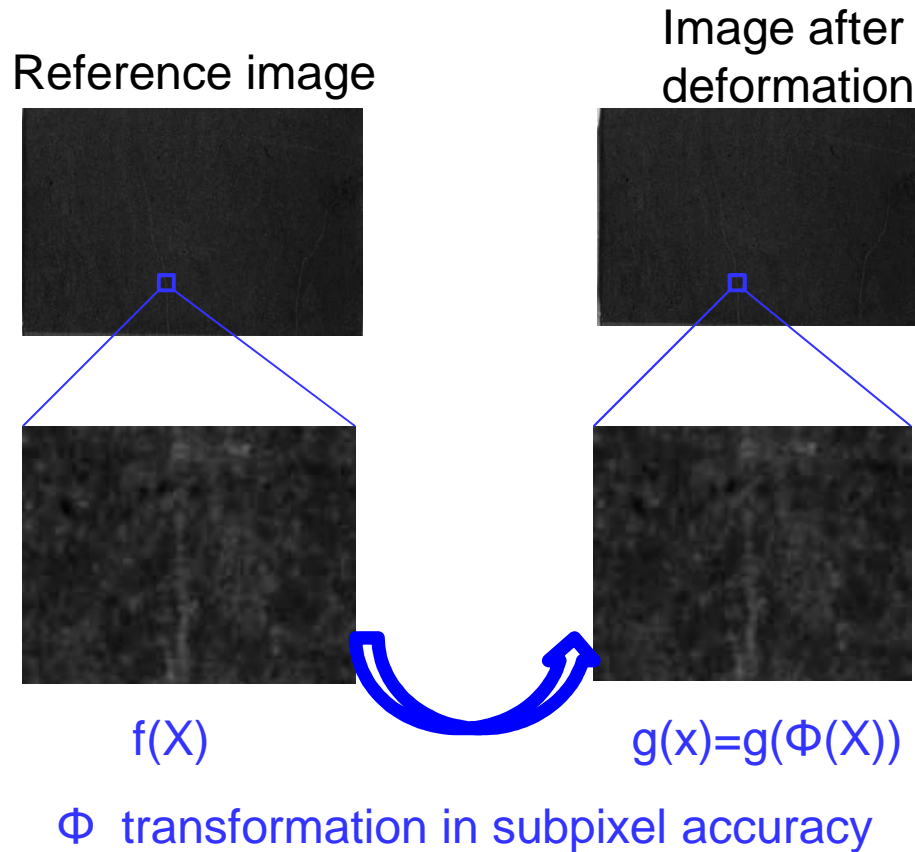
Uniaxial compression under controlled moisture with multiscale full-field strain measurements

- ❖ Loading device
- ❖ Macroscopic measurements : strain gauges, LVDT
- ❖ Suction control
- ❖ Optical multiscale full-field strain measurements during hydric-mechanical loading



**Macroscopic optical setup (24x36 mm)
& Microscopic optical setup (1.5x1.5 mm)**

Digital image correlation (DIC) and associated errors



Digital image correlation

Identify the position of each object point in two images by correlation algorithm

$$\Phi_D \approx \underset{\Phi_0 \in V}{\operatorname{Argmin}} C(f, g, D, \Phi_0)$$

Example::

$$C(\Phi_0) = \int_D [f(u) - g(\Phi_0(u))]^2 du \approx \sum_{ij \in D} [f(u_{ij}) - g(\Phi_0(u_{ij}))]^2$$

Determination of the local (full-field) or average strains

Average the transformation gradient over domains of interest

Various sources of random or systematic errors

Noise, image quality, **contrast**, **interpolation method**, **out-of-plane motion**, etc.

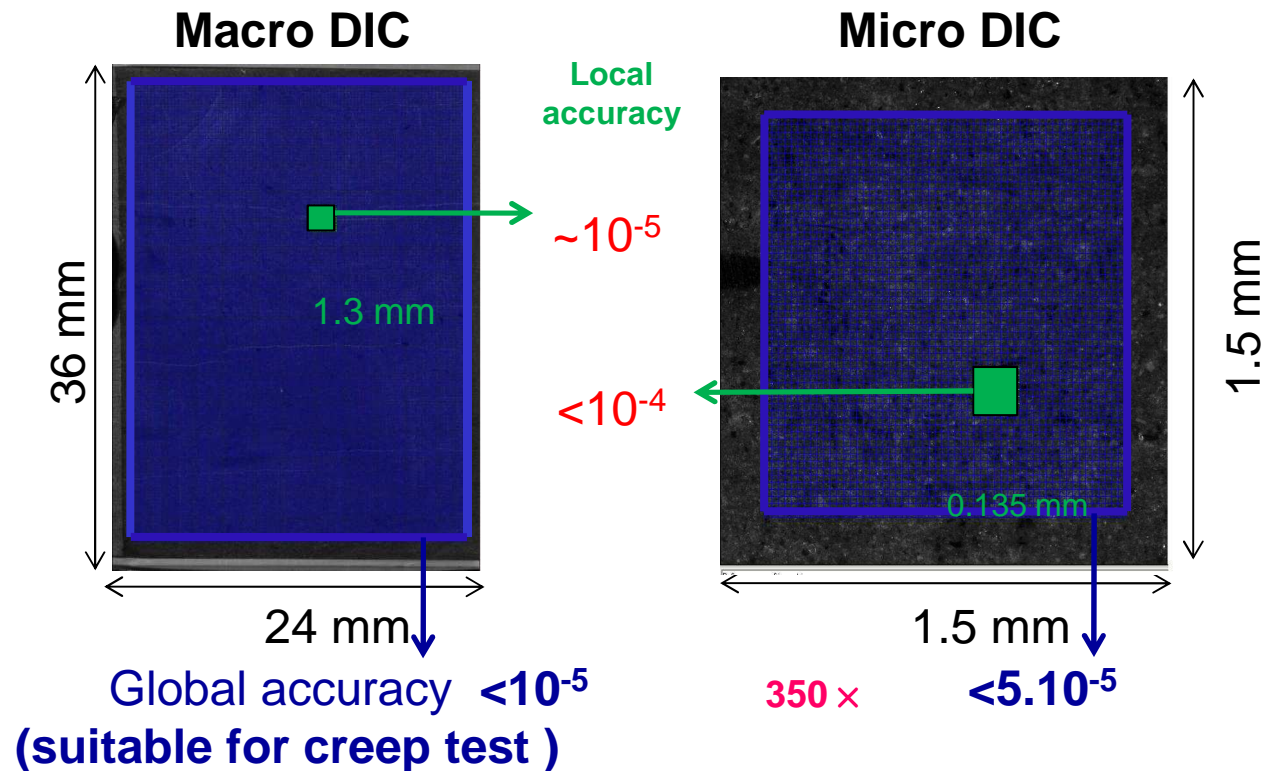
Improvement of the system (Yang and Michel *et al.* 2010)

Optimal aperture minimizes the systematic errors

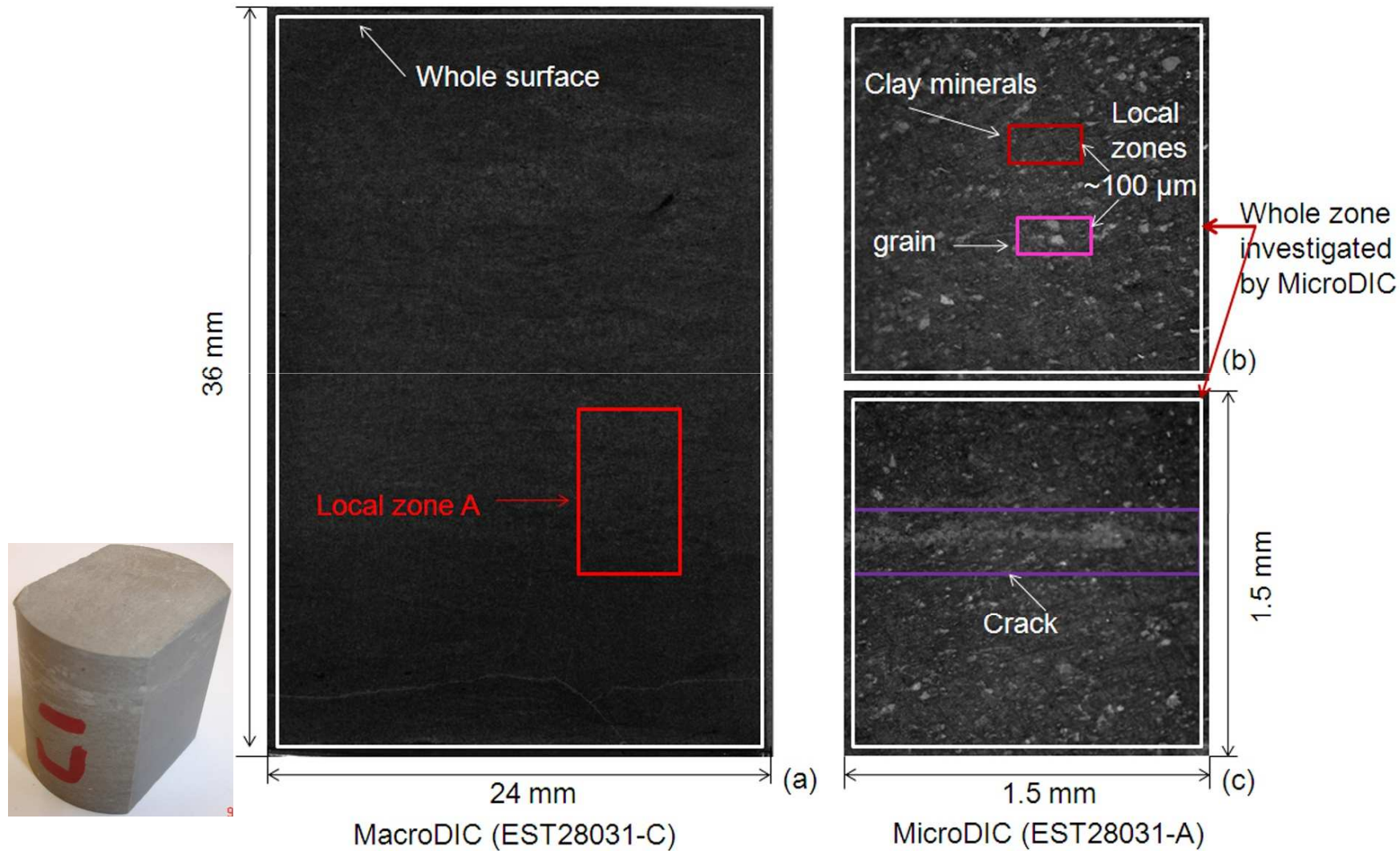
Minimizing the effect of global out-of-plane motion

$$\varepsilon = \varepsilon_a - \Delta g/g1 \quad (\Delta g/g = -dZ/OC \quad \Delta Z^{\text{macro}} = \Delta Z^{\text{micro}} + D \varepsilon^{zz})$$

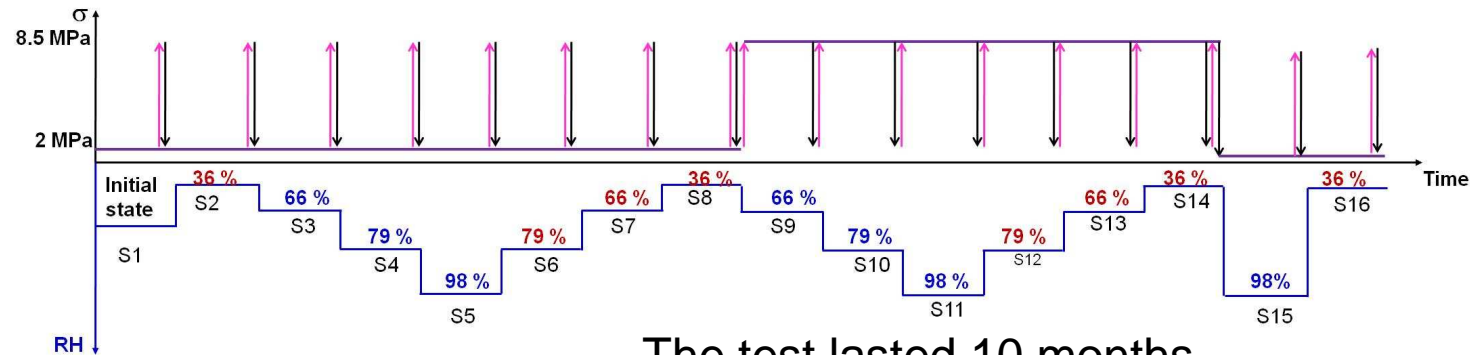
Strain measurement & accuracy



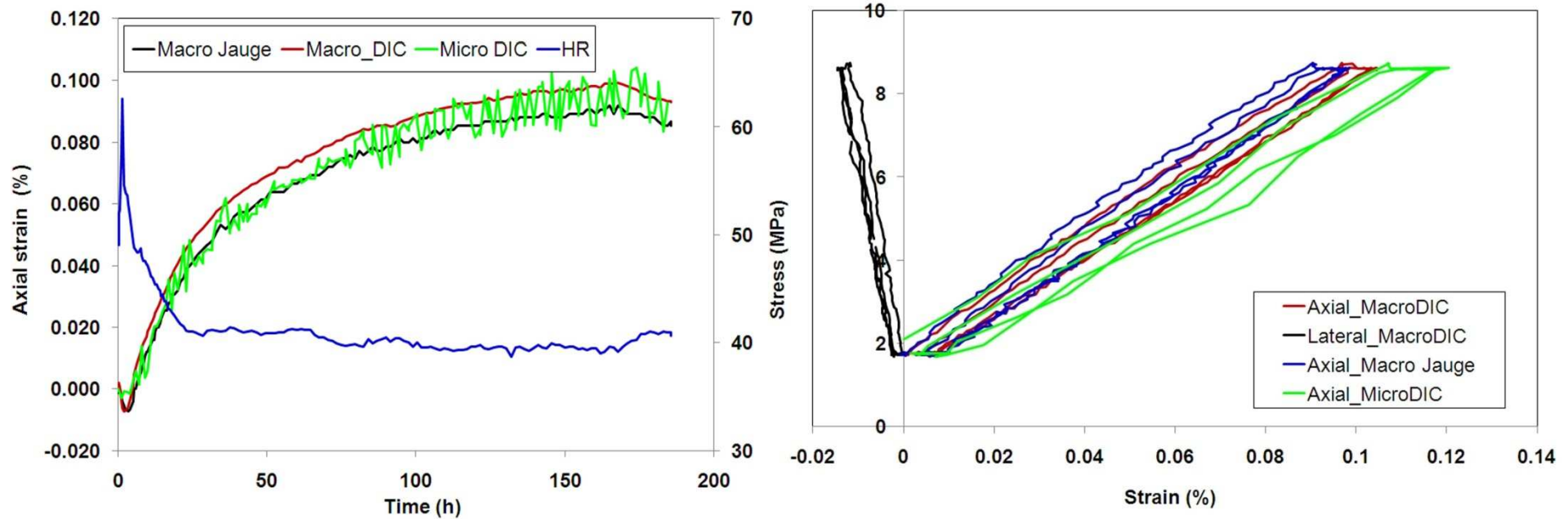
Characterization of the heterogeneity



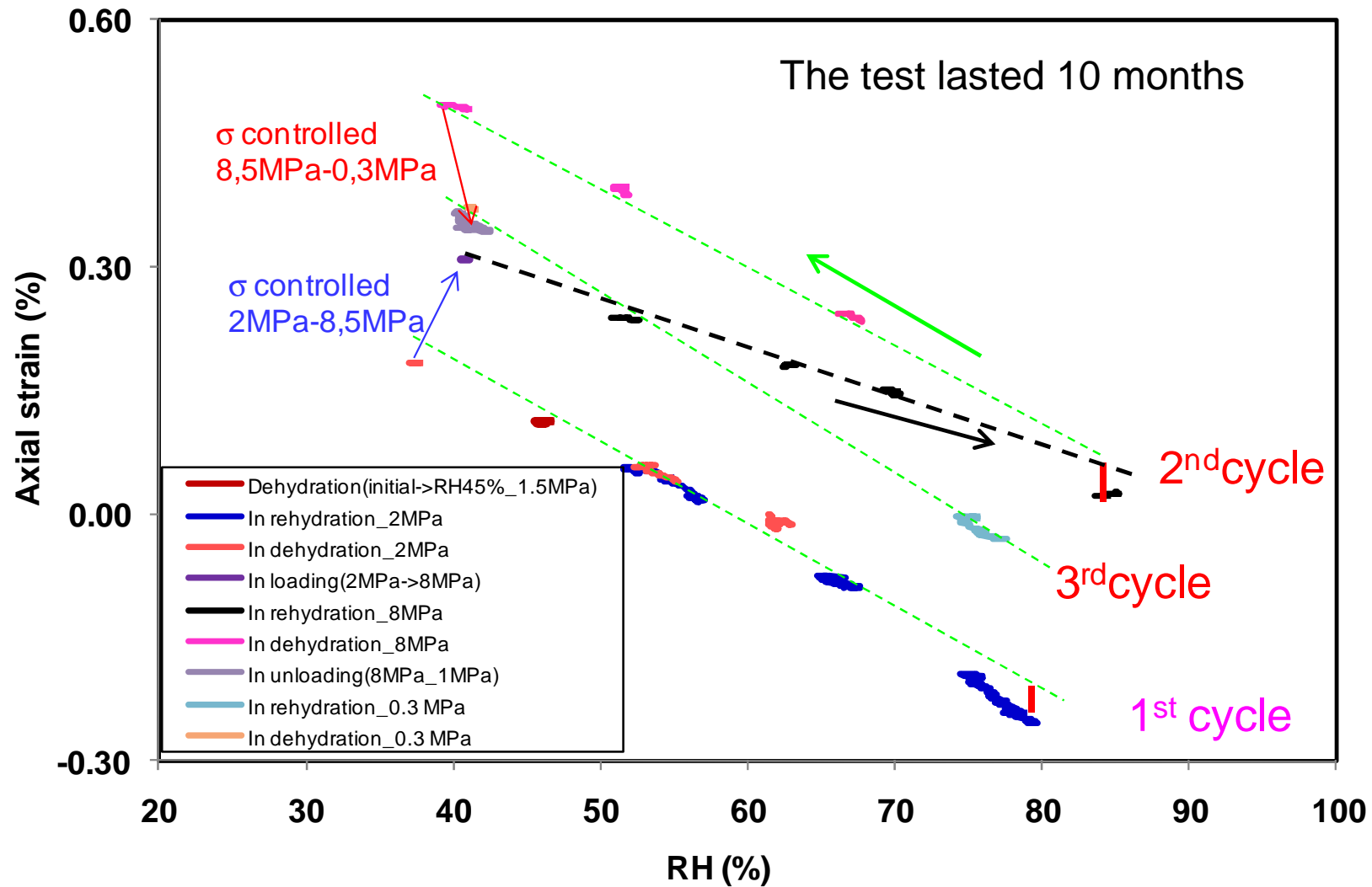
Hydration and dehydration under uniaxial stress (Yang and Michel et al. 2011, in preparing)



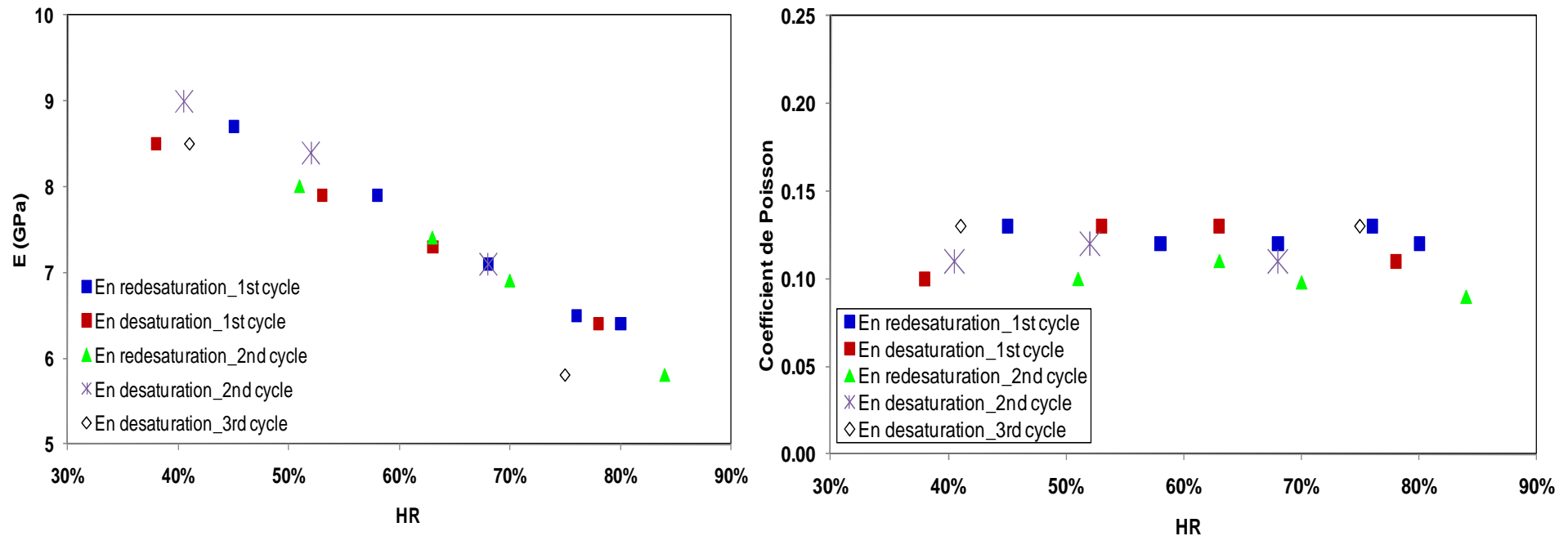
The test lasted 10 months



Hydration and dehydration under uniaxial stress

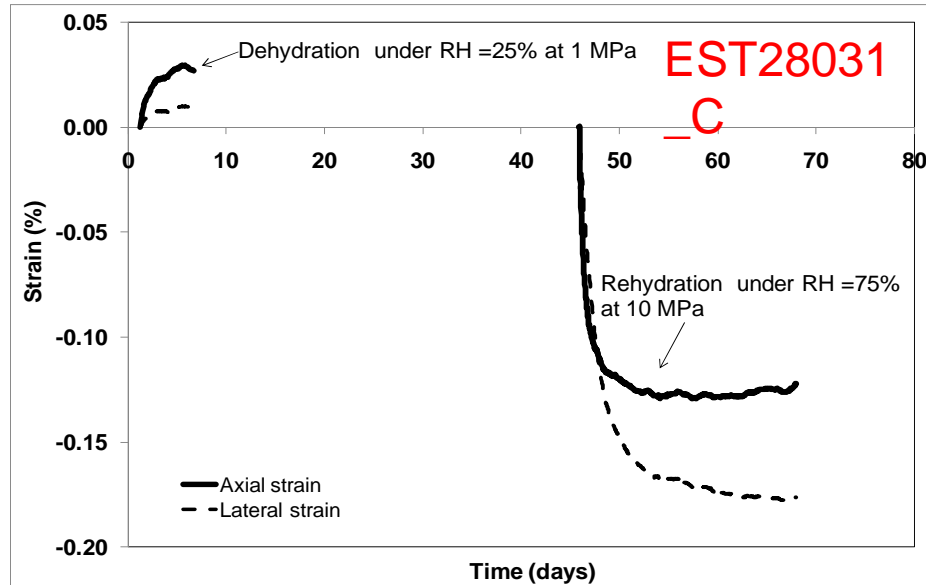


Hydration and dehydration under uniaxial stress



ϵ vs RH quasi-linear ,
reversible under low σ
and irreversible under high σ

E vs RH quasi-linear
 ν vs RH quasi-constant
for RH < 85%

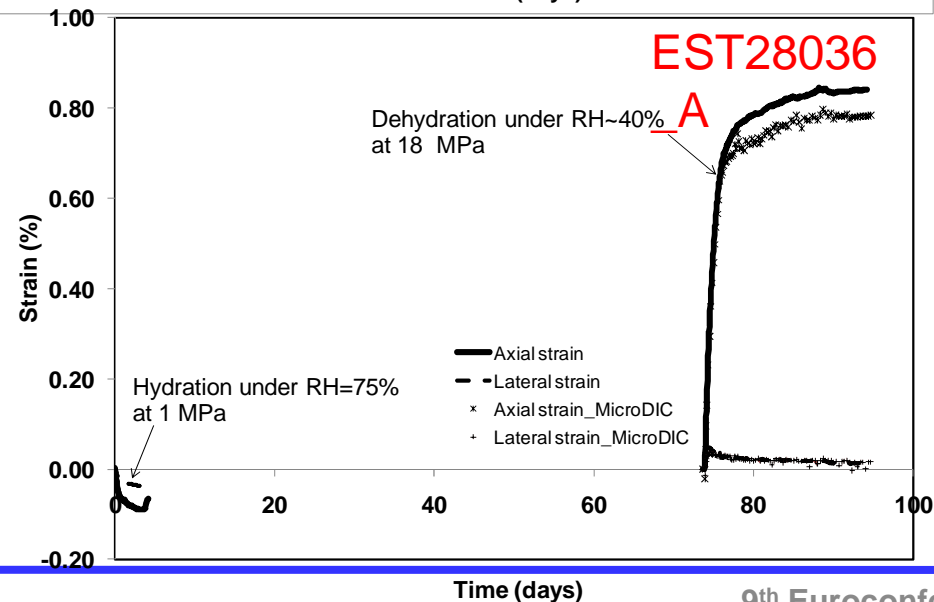


$$\epsilon_{\text{lateral}}/\epsilon_{\text{axial}} \sim 0.3$$

at 1 MPa

$$\epsilon_{\text{lateral}} = -0.18\% > \epsilon_{\text{axial}} = -0.13\%$$

at 10 MPa
during rehydration

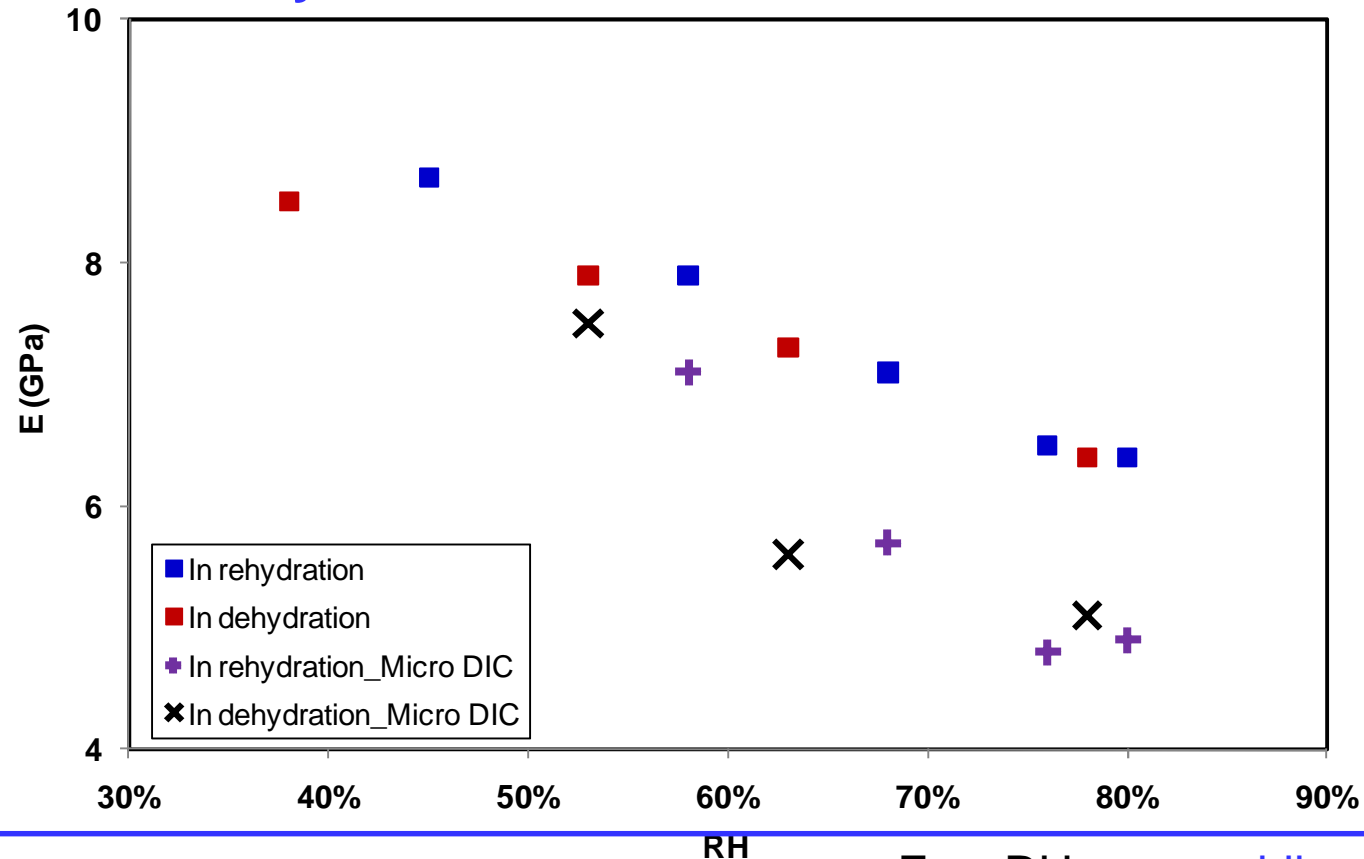


$$\epsilon_{\text{lateral}} = 0.08\% < \epsilon_{\text{axial}} = 0.83\%$$

at 18 MPa
during dehydration

Shrinkage and swelling strongly
depend on the applied stress
The classical Biot theory is not
relevant

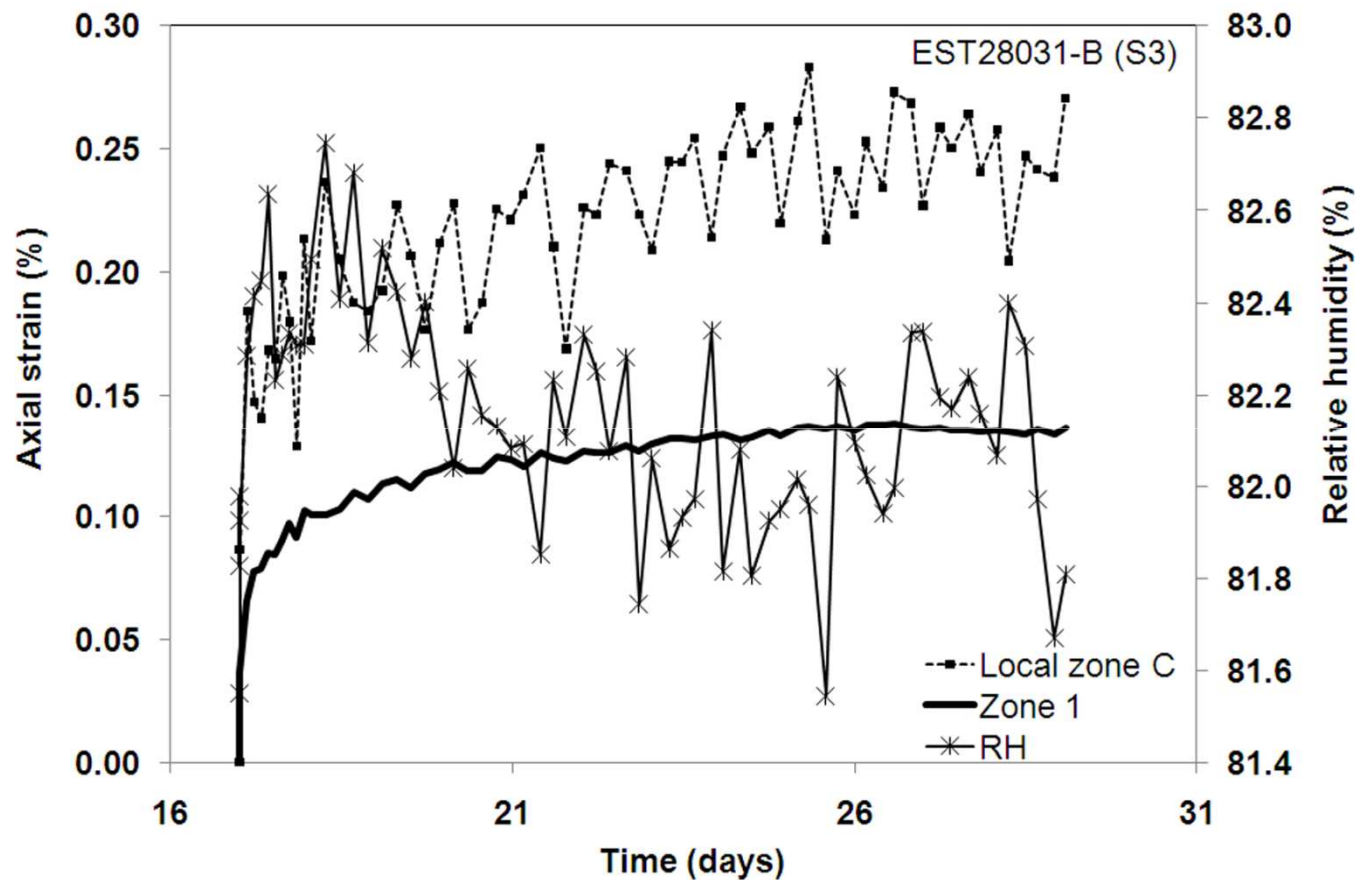
Hydration and dehydration under uniaxial stress



ε vs RH quasi-linear ,
reversible under low σ
and irreversible under high σ

E vs RH quasi-linear
 ν vs RH quasi-constant
for RH < 85%

Strain at various scales



Local zone with high
clay content (200 μm)

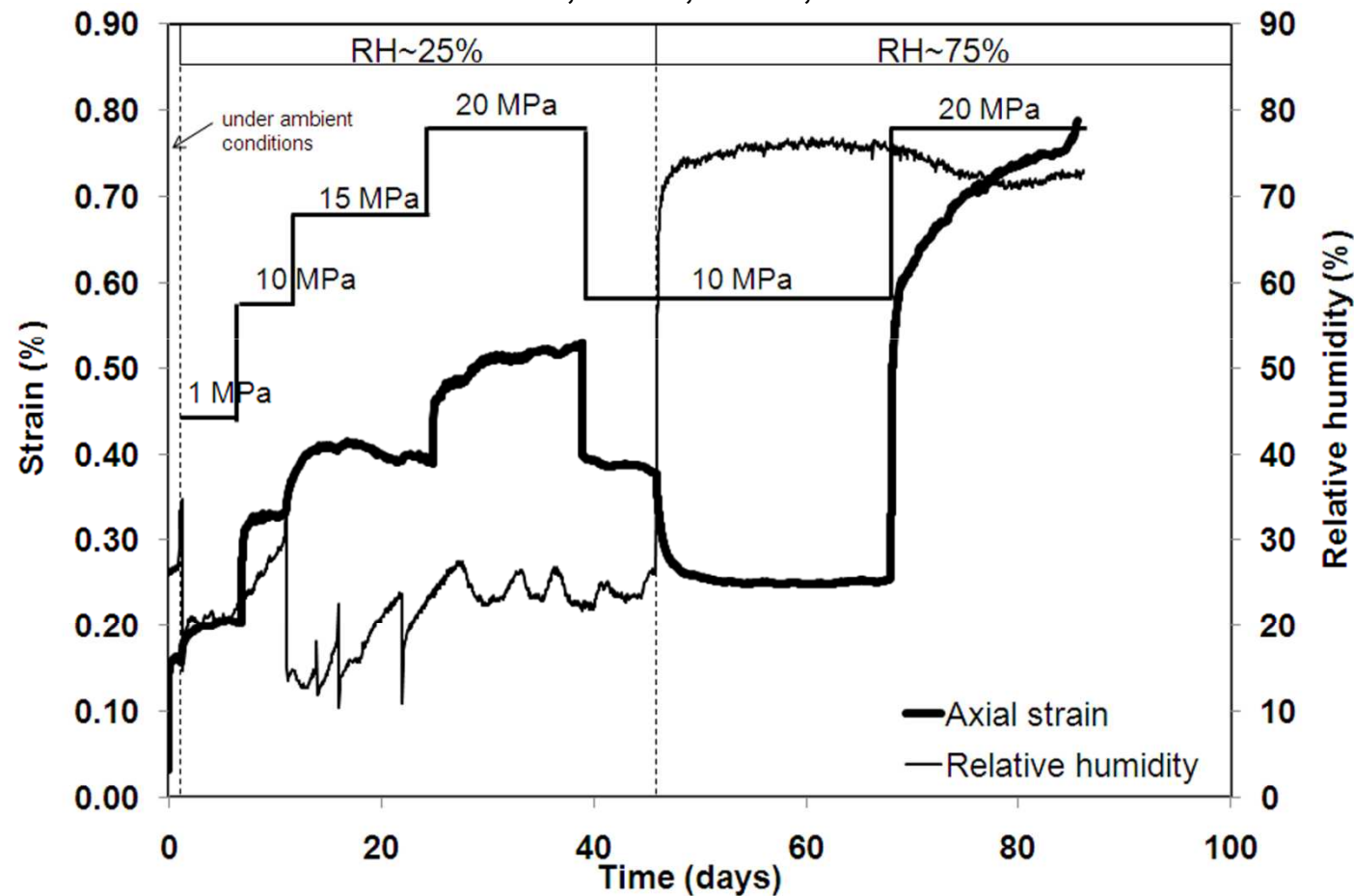
Zone 1
(millimetric scale)

$\Delta\epsilon$ (local zone) $\approx 10 \times \Delta\epsilon$ (Zone 1)
Subjected to ΔRH

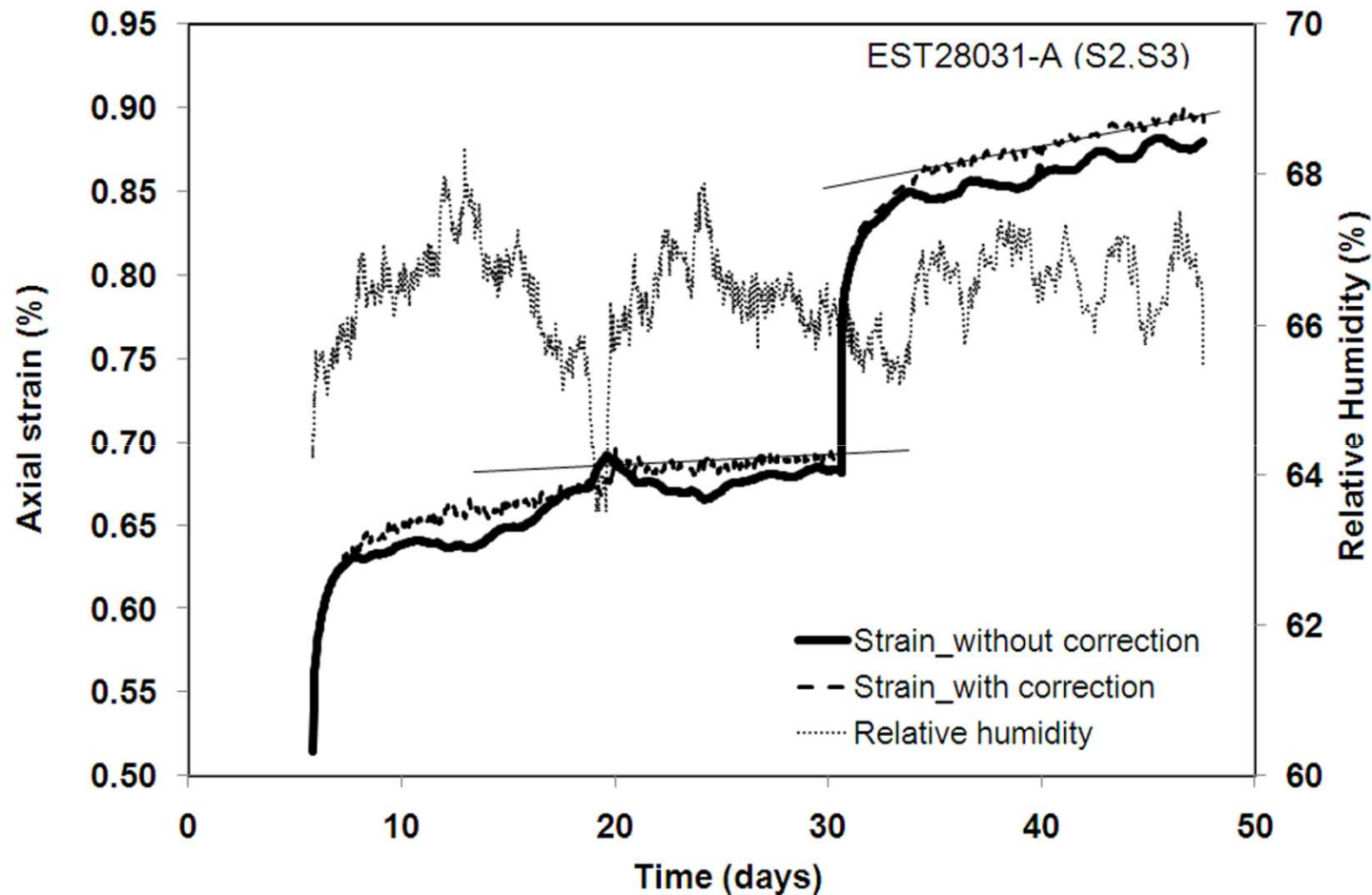
Creep behavior under controlled HM (Yang and Michel *et al.* 2011)

Loading paths: axial stress 10 MPa; 15 MPa; 20 MPa

RH 25%; 65%; 75%; 80%

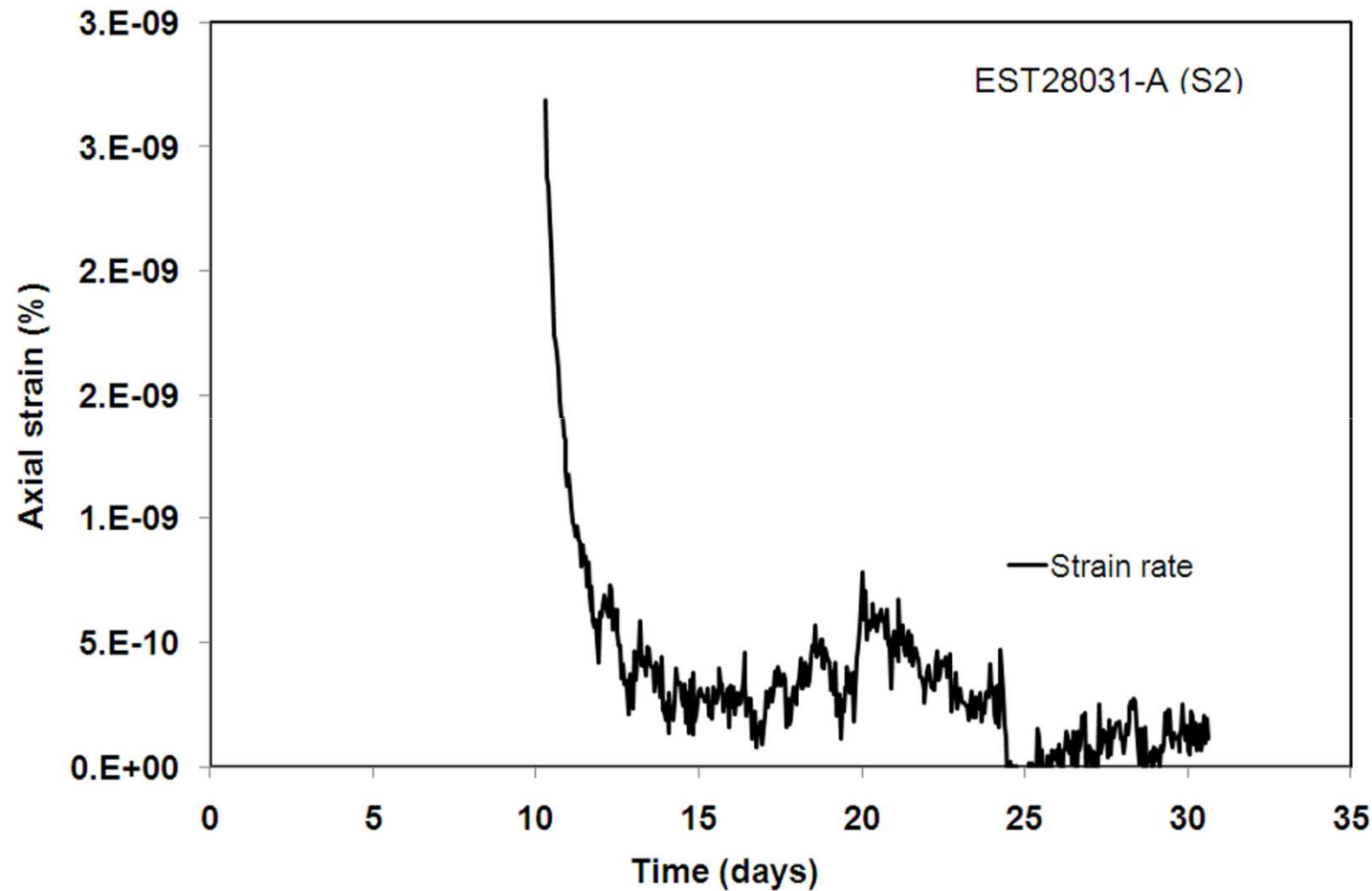


Characterization of strain rate



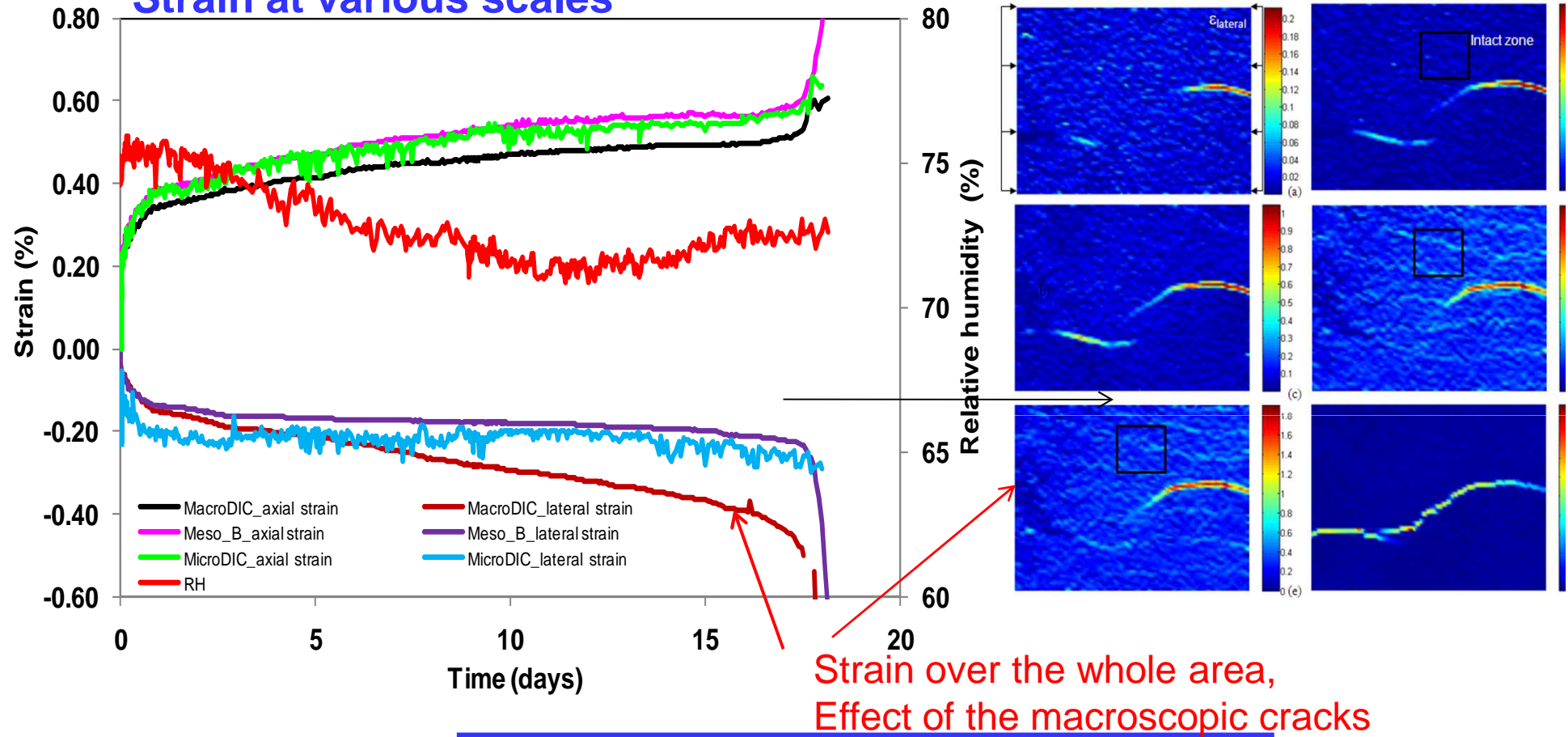
Correction of the strain using the linear relation between ε and RH

Strain rate over time



2 weeks
last 4 days

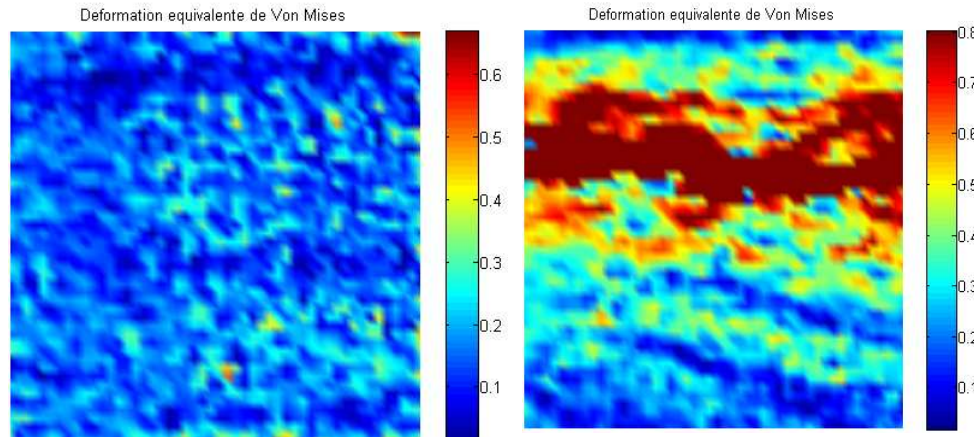
Strain at various scales



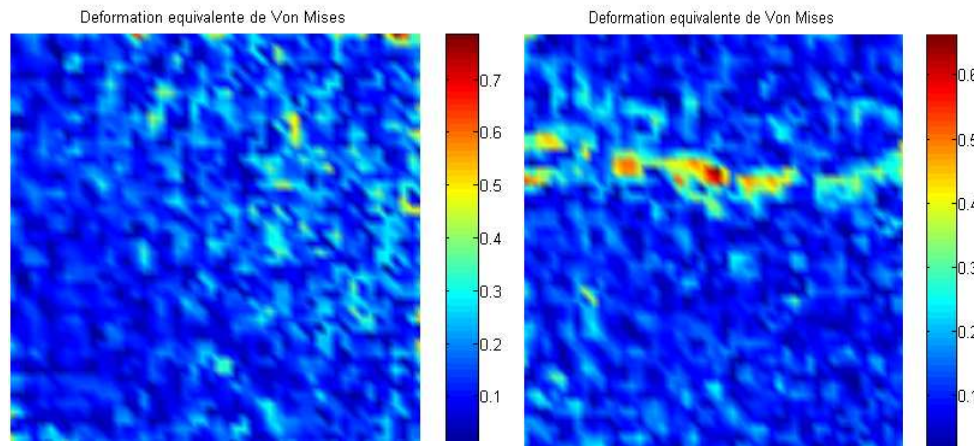
RH and/or $\sigma \nearrow$ strain rate \nearrow

Strain rate 10^{-9} s^{-1} (18 MPa) - 10^{-11} s^{-1} (9 MPa)

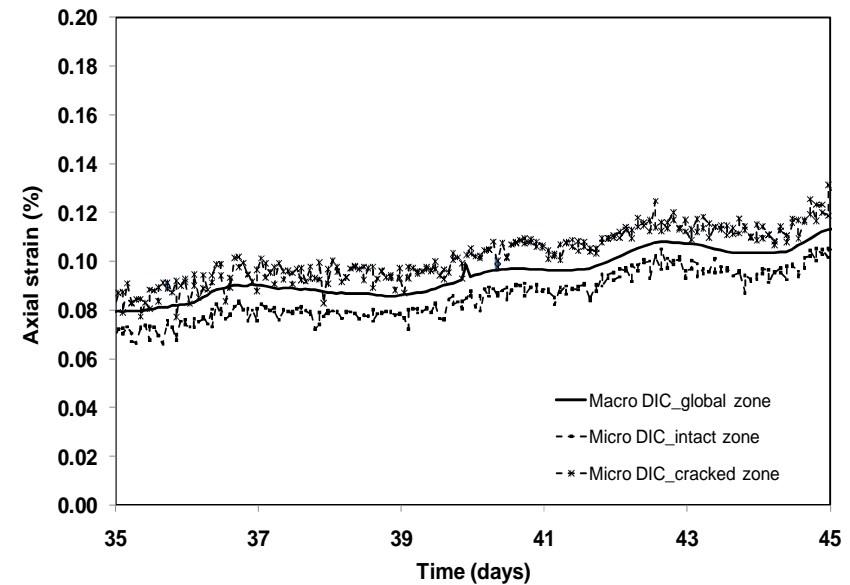
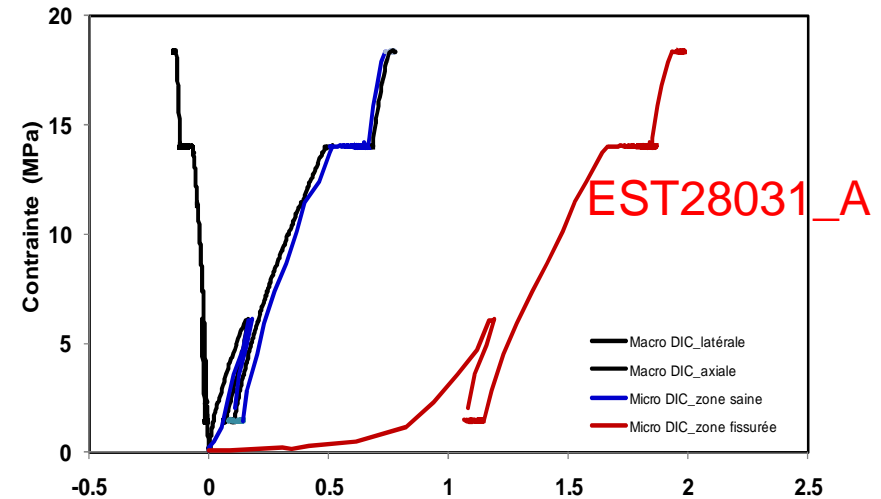
Crack perpendicular to the stress direction



Map of ϵ_{eq} σ from 1 MPa to 7 MPa



Map of ϵ_{eq} $\sigma = 18$ MPa (30th – 35th day)



Hydromechanical behavior of the unsaturated clayey rocks

Mechanical behavior

$\sigma - \varepsilon$ linear $\sigma < 10\text{MPa}$

$E - HR$ linear, reversible under $RH < 85\%$

Poisson's ratio constant = 0,13

Shrinkage and swelling

$\varepsilon - HR$ linear and reversible $< 85\%$, irreversible at high σ

Small damage $> 85\%$

Shrinkage and swelling strongly depend on the applied stress

Classical Biot model is not relevant

Creep behavior under controlled RH

HR and /or σ \nearrow Strain rate \nearrow
Strain rate 10^{-9} s^{-1} (18 MPa)- 10^{-11} s^{-1} (9 MPa)

Areas with cracks perpendicular to the applied loads had a strain rate similar to that of intact zones

Cracks parallel to the applied stress developed and opened over time and could lead to fracture.

Thank you for your attention